AGU ADVANCING EARTH AND SPACE SCIENCE

JGR Biogeosciences

DATA ARTICLE

10.1029/2022JG007101

Reconstructing Long-Term Forest Cover in China by Fusing National Forest Inventory and 20 Land Use and Land Cover Data Sets

Xiaosheng Xia[1,2], Jiangzhou Xia[3], Xiuzhi Chen[1,2], Lei Fan[4], Shuguang Liu[5], Yuanwei Qin[6], Zhangcai Qin[1,2], Xiangming Xiao[6], Wenfang Xu[1,2], Chao Yue[7], Xu Yue[8], and Wenping Yuan[1,2]

[1]School of Atmospheric Sciences, Sun Yat-sen University, Zhuhai, China, [2]Southern Marine Science and Engineering Guangdong Laboratory, Zhuhai, China, [3]Tianjin Key Laboratory of Water Resources and Environment, Tianjin Normal University, Tianjin, China, [4]School of Geographical Sciences, Southwest University, Chongqing, China, [5]College of Life Science and Technology, National Engineering Laboratory for Applied Technology in Forestry & Ecology in South China, Central South University of Forestry and Technology, Changsha, China, [6]Department of Microbiology and Plant Biology, Center for Earth Observation and Modeling, University of Oklahoma, Norman, OK, USA, [7]State Key Laboratory of Soil Erosion and Dryland Farming on the Loess Plateau, Northwest A&F University, Yangling, China, [8]Jiangsu Key Laboratory of Atmospheric Environment Monitoring and Pollution Control, Collaborative Innovation Center of Atmospheric Environment and Equipment Technology, School of Environmental Science and Engineering, Nanjing University of Information Science and Technology (NUIST), Nanjing, China

Xiaosheng Xia and Jiangzhou Xia contributed equally to this work.

Key Points:

- We reconstructed long-term Chinese forest cover maps by combining national forest inventory and 20 land use and land cover data sets
- The reconstructed forest cover maps reproduced well Chinese forest change consistent with national forest inventory
- Reconstructed forest maps provide the distribution of various forest types in China

Supporting Information:

Supporting Information may be found in the online version of this article.

Correspondence to:

W. Yuan,
yuanwpcn@126.com

Citation:

Xia, X., Xia, J., Chen, X., Fan, L., Liu, S., Qin, Y., et al. (2023). Reconstructing long-term forest cover in China by fusing national forest inventory and 20 land use and land cover data sets. *Journal of Geophysical Research: Biogeosciences*, *128*, e2022JG007101. https://doi.org/10.1029/2022JG007101

Received 19 JUL 2022
Accepted 14 MAR 2023

Author Contributions:

Conceptualization: Jiangzhou Xia, Wenping Yuan
Formal analysis: Jiangzhou Xia
Methodology: Xiaosheng Xia, Wenping Yuan
Supervision: Wenping Yuan
Validation: Yuanwei Qin, Xiangming Xiao
Visualization: Xiaosheng Xia
Writing – original draft: Xiaosheng Xia, Wenping Yuan
Writing – review & editing: Xiaosheng Xia, Jiangzhou Xia, Xiuzhi Chen, Lei Fan, Shuguang Liu, Yuanwei Qin, Zhangcai Qin, Xiangming Xiao, Wenfang Xu, Chao Yue, Xu Yue, Wenping Yuan

Abstract As an important type of terrestrial carbon sink, forests play a critical role in offsetting anthropogenic fossil fuel CO_2 emissions which should help nations to achieve carbon neutrality goals worldwide. According to National Forest Inventory (NFI), China has experienced substantial increases in forest cover by benefiting from national afforestation projects initiated in the 1980s. However, none of the current land use and land cover (LULC) data sets can reproduce the long-term changes of forest cover derived from NFI in China. Here, by combining NFI and 20 LULC data sets, we developed a new method of reconstructing historical forest cover in China from 1980 to 2015 at 5-year intervals. The new forest cover data set can accurately reproduce the historical changes of forest cover in China during this period. Validated against 3851 field survey samples covering the study period of 1985–2015, the data sets show high accuracy with overall accuracy varying from 76.9% to 99.4%. Accurate long-term forest cover maps have great potential for use in estimating terrestrial carbon, tracking forest management, and other scientific research studies.

Plain Language Summary Planting trees can absorb carbon dioxide from the atmosphere and mitigate global warming. Benefiting from the national afforestation projects initiated in the early 1980s, forests in China have grown significantly. However, these land cover maps, based on remote sensing satellite observations, do little to reproduce this remarkable greening change. Therefore, we produced a new forest map data set for China from 1980 to 2015 by combining the statistical forest area and up to 20 different remotely sensed land cover maps at 5-year intervals. The new forest map data set has a high validation accuracy and reproduces the greening process in China well. Accurate long-term forest maps are essential to better understanding the potential of trees to mitigate climate change through CO_2 uptake.

1. Introduction

As one of the most important terrestrial carbon sinks, forests play a critical role in regulating global and regional carbon budgets (Houghton & Nassikas, 2018; Le Noë et al., 2021). Previous studies have estimated a global forest sink of 2.4 Pg C yr^{-1} for 1990 to 2007 (Pan et al., 2011), which contributes a large fraction of the entire terrestrial sink globally (Friedlingstein et al., 2020). The Chinese government has committed to reaching carbon neutrality by 2060 (NDRC, 2021), which means the various ecosystem carbon sinks and carbon capture and storage need to offset all fossil fuel CO_2 emissions (Rogelj et al., 2015). In China, forest ecosystems also dominate the terrestrial carbon sink, contributing 80% of terrestrial carbon sinks and 39% of terrestrial carbon stocks while providing a least 2.97 Pg C of potential carbon sequestration for 2010 to 2030 (Fang et al., 2018; Tang et al., 2018). In addition, the identification of forest types is also important for simulating carbon sinks because ecosystem models set different model parameters for various forest types (Houghton et al., 1983). For example, the leaf turnover rate of boreal conifer deciduous forests was twice that of boreal conifer evergreen forests (Ryan & Law, 2005), which substantially impacts the amount of aboveground litterfall. Since accurate information of forest cover with forest types is critical for reducing the uncertainty in estimating China's forest carbon balance and better understanding its role in potential carbon sequestration, an urgent need exists to produce cover maps of China's forests.

Although numerous studies have produced land use and land cover (LULC) data sets (Liu et al., 2021), large differences of forest area in China remain among various data sets. Qin et al. (2015) reported that the forest area estimations of five LULC data sets ranged from 174×10^4 km^2 to 227×10^4 km^2 in 2010, with a 29% difference of forest cover percentage among these data sets. Similarly, Yang and Huang (2021) compared the forest area estimations in China derived from three LULC data sets and indicated that the difference of forest area estimations is up to 78×10^4 km^2 in 2015, which are account for 35% of corresponding forest area statistics in national forest inventory (NFI) reports.

China currently has the world's largest area of afforestation, benefiting from several afforestation and reforestation projects dedicated to improving ecological conditions that had deteriorated previously (Fang et al., 2001; FAO, 2016; Yuan et al., 2014). The forest area has substantially increased from 115×10^4 km^2 in the 1980s to 220×10^4 km^2 around 2015 according to NFI data (State Forestry Bureau, 2019). It was also reported that the forest area in Asia shifted from a net loss during 1990–2000 to a major net gain during 2000–2010, mainly due to the ongoing afforestation in China (FAO, 2016). However, long-term satellite-based LULC data sets have shown challenges to reproduce these significant forest increases in China (Yang & Huang, 2021), and major discrepancies of forest area exist between data sets derived from satellite-based LULC data and statistical reports (Schepaschenko et al., 2015). Yang and Huang (2021) reported that forest area in China only increased by 4.34% from 1985 to 2019, while Hansen et al. (2013) even witnessed a 3.87×10^4 km^2 net loss during 2000–2012 according to satellite observations. Although several LULC data sets produced since the 1980s exist that cover long-term time series (Liu et al., 2021), no studies have investigated to see if these data sets can indicate substantial increases of forest areas observed during the past decades.

NFI is identified as a critical national infrastructure for providing forest cover and biomass storage (Zeng et al., 2015). Since the second nationwide NFI was implemented from 1977 to 1981 (i.e., NFI2), the standard sampling and survey methods were used for the whole country (Zeng et al., 2015). Subsequently, the other seven NFIs (NFI3 to NFI9) were continuously implemented with about a 5-year cycle (Lin et al., 2013). Benefiting from a large volume of samples across entire China, the forest area derived from NFI has been considered the reference data set (State Forestry Bureau, 2003). Previous studies used the NFI data set to estimate forest carbon budget (Fang et al., 2001; Piao et al., 2009). However, NFI only provided province-level forest area, which limits the applications of terrestrial ecosystems for simulating carbon dynamics (Yuan et al., 2014). Therefore, a very urgently needed task is to produce long-term forest cover maps consistent with NFI as a basic data set for ecosystem modeling to robustly evaluate the changes of terrestrial carbon sinks and drivers.

This study aims to classify forest cover in China by combining several current LULC data sets; in particular, we reconstructed long-term forest cover maps starting from the early 1980s. The objectives of this study are to (a) develop a new method combining multiple LULC data sets and generate new forest cover maps covering China; (b) identify and provide maps of the distribution of the forest types, and (c) investigate the forest gain and loss in China during the past three decades.

2. Materials and Methods

2.1. Data Sets

2.1.1. National Forest Inventories

To investigate the area, composition, and distribution of forest resources, the State Forestry Bureau of China launched nine national forest inventories (NFIs) in 1973–1976, 1977–1981, 1984–1988, 1989–1993, 1994–1998, 1999–2003, 2004–2008, 2009–2013, and 2014–2018 (State Forestry Bureau, 2019). Forest areas, which are composed of needleleaf forests, broadleaf forests, bamboo, and economically important plantation forests, at the province scale during the 2nd–9th NFIs were employed in this work.

2.1.2. Land Use and Land Cover Datasets

Twenty LULC data sets were employed as the fundamental data sources for forest cover reconstruction (Table 1). Forest cover was derived from these LULC data sets, and then masked, re-projected, and aggregated into the unified spatial extent for China with spatial reference to GCS_WGS_1984 and using a spatial resolution of 0.01°.

Table 1
Land Use and Land Cover Data Sets Employed in This Study

Datasets	Resolution	Time range	Source
NFDM[a]	100 m[b]	1977–1981, 2014–2018	http://www.forestdata.cn
CGLS_LC	100 m	2015	Buchhorn et al. (2020)
CLCD	30 m	1985, 1990–2015[c]	Yang and Huang (2021)
CLUD	1 km	1980, 1990, 1995, 2000, 2005, 2010, 2015	Liu et al. (2005)
ESACCI_LC	300 m	1992–2015[c]	ESA (2014)
FROM_GLC	10 m	2017	Gong et al. (2019)
GFC30[a]	30 m	2018	Zhang et al. (2020)
GFC[a]	30 m	2000, 2012	Hansen et al. (2013)
GLASS_GLC	5 km	1982–2015[c]	Liu et al. (2020)
GLC2000	1 km	2000	Bartholomé and Belward (2005)
GLC_FCS30	30 m	1985, 1990, 1995, 2000, 2005, 2010, 2015	Zhang et al. (2021)
GLCNMO	1 km	2003, 2008, 2013	Tateishi et al. (2011)
GlobCover	300 m	2009	Bontemps et al. (2010)
GlobeLand30	30 m	2000, 2010	Chen et al. (2015)
Li_Forest[a]	30 m	Circa 2010	Li et al. (2014)
MODIS	500 m	2001–2015	Friedl et al. (2010)
MLUD	250 m	2005	Ge et al. (2018)
UMD_LC	1 km	1992	Hansen et al. (2000)
Wang_LC	250 m	2001, 2010	Wang et al. (2015)
Wu_LC	100 m[b]	1980s	http://www.resdc.cn

[a]These data sets only contain forest class and don't contain other forest sub-type. [b]These data sets originally were digitalized maps and were later rasterized at a 100 m spatial resolution. [c]These data sets were updated annually, and other data sets were only updated at several points in time.

For the conversion from the data sets with the finer resolution, the 0.01° grid pixel was defined as forest if over 50% of finer grids within this pixel are clarified as forest in the original data set.

2.1.3. Satellite-Based Vegetation Index Data Set

We downloaded the third generation Global Inventory Modeling and Mapping Studies (GIMMS-3g) Normalized Difference Vegetation Index (NDVI) data sets with a spatial resolution of 8 km and temporal resolution of 15-day during 1982–2015 from https://ecocast.arc.nasa.gov. The maximum NDVI of the growing season within about 5-year forest inventory periods was applied as a priority proxy to determine how many potential forest pixels were identified as forests under the same level of consistency.

2.1.4. Climate Zone Mapping

In general, needleleaf forests are mainly evergreen, except for Larix needleleaf forests, which are deciduous and mainly located in the boreal zone. Broadleaf forests are mainly deciduous, except for tropical and subtropical broadleaf forests, which are evergreen. Therefore, a climate zone map, accessible from the Resource and Environment Science and Data Center (http://www.resdc.cn), was applied to further distinguish evergreen and deciduous forest types. The original map of climate zones, which consisted of 12 temperature zones, 24 humidity regions, and 56 climatic subzones, was integrated into four main temperature zones (boreal, temperate, subtropical, and tropical zones) for forest reconstruction.

2.2. Reconstruction Method of Historical Forest Cover in China

This study developed a new method of reconstructing historical forest cover maps from 1980 to 2015 by integrating multiple readily available LULC data sets (Figure 1). Since different input data, especially for LULC and NFI data, have different time-spanning, it is important to match them into a consistent time point (Figure

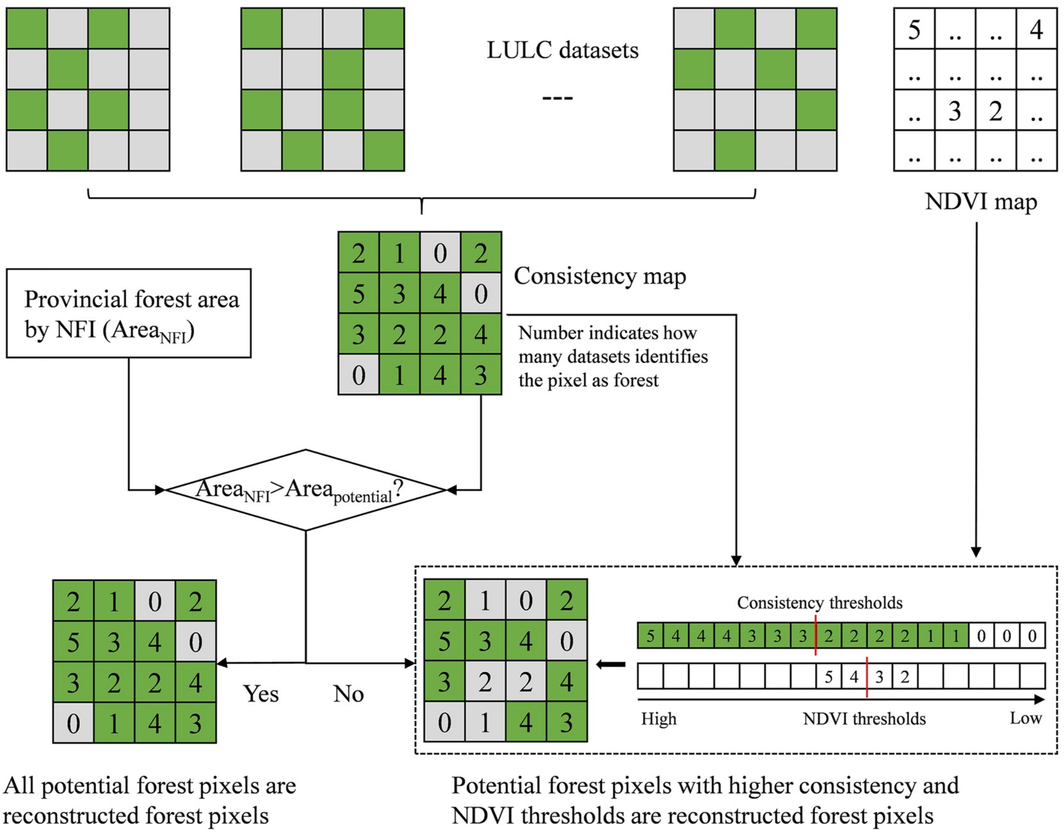

Figure 1. Methodology flow chart in the forest reconstruction. The green squares denote forest pixels and the gray ones denote non-forest pixels. NFI represents national forest inventory and land use and land cover (LULC) represent LULC data sets. $Area_{potential}$ denotes the total area of all potential forest pixels.

S1 in Supporting Information S1). For each study period, we overlaid all available LULC data sets to calculate the spatial agreement or consistency of forest cover at each pixel, and the consistency (CON) is defined by how many existing data sets classify the investigated pixel as forest (Figure S2 in Supporting Information S1). An investigated pixel was identified as forest cover by more LULC data sets (i.e., higher consistency), and then the pixel had a larger probability to be identified as the forest (Fang et al., 2020). To determine the threshold of consistency for identifying forest, all pixels with positive CON (CON > 0) were selected as the potential forest pixels, and they were sorted by descending CON. The pixels at the front of the queue had higher consistency and larger possibility to be identified as the forest. Forest areas derived from the NFI data set were used to determine the CON thresholds for each province (Figure S3 in Supporting Information S1). Specifically, there were two conditions, and we used different strategies to determine the CON thresholds. First, if the total area of all potential forest pixels (CON > 0) was less than the forest area statistics of NFI in a given province, we considered all potential forest pixels as forest and leave the gap of forest area being unfilled. Therefore, the area of the identified forest cover was underestimated. Second, if the area of all potential forest pixels (i.e., CON > 0) was larger than the reported NFI forest area, we calculated the total area of pixels with the same level of consistency, and then accumulated the pixels' area of different levels of consistency from the maximum to the minimum. When the reported NFI forest areas (A_{NFI}) were larger than the accumulated areas of CON ≥ m, but less than the accumulated area of CON ≥ m-1 (i.e., A_{id1}), the *m* was determined as the thresholds of consistency and all pixels with CON ≥ m were identified as the forest. However, it should be noticed that the rest forest area (A_{NFI}-A_{id1}) should still be identified from the pixels with CON = m-1. We hypothesized that under the same level of consistency, a higher NDVI value suggests a larger probability of a pixel actually being forest cover. Similarly, we calculated the maximum NDVI of the growing season ($NDVI_{max}$) at the consistency level of m-1 within about 5-year inventory periods and sorted the pixels by descending $NDVI_{max}$. We selected *n* pixels at the front of the queue as the rest forest pixels, and make sure their total area was the closest to the area of A_{NFI}-A_{id1}. A forest pixel was identified as a pixel with a relatively high consistency between LULC data sets and with a relatively high NDVI value, and

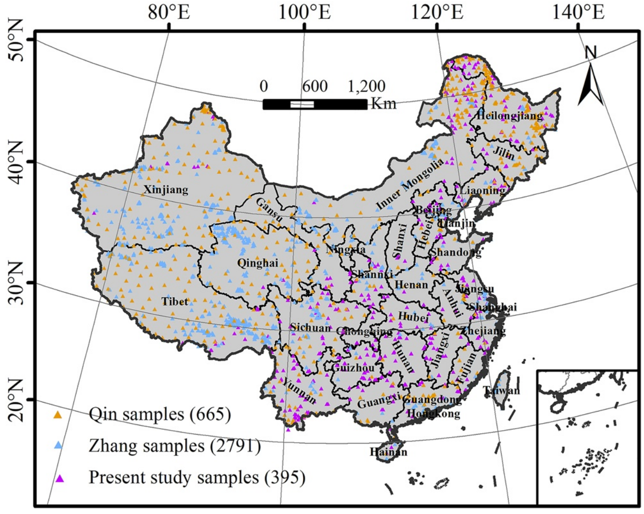

Figure 2. Locations of forest field samples used in this study for accuracy assessment based on 395, 665, and 2791 field samples collected in this study, by Qin et al. (2015) and by Zhang et al. (2021), respectively.

the total area of all identified forest pixels should equal the statistical forest area in the investigated province.

Theoretically, we could use the same method described above to classify the forest types into evergreen needleleaf, evergreen broadleaf, deciduous needleleaf, and deciduous broadleaf forests. However, the availability of the LULC data sets limited the application of the same reconstruction method to these four forest types, because only a few LULC data sets exist that provide the distribution of these four forest types in several periods, especially before the 2000s. For example, only one of the available data sets provided the distribution of needleleaf and broadleaf forests in 1985, and none provided the distribution of evergreen and deciduous forests in 1980. Therefore, this study assumed the spatial distribution of these four forest types did not change temporally. NFI data sets provide the area of needleleaf ($Area_{need}$) and broadleaf forests ($Area_{broa}$), but not for evergreen and deciduous forests. Therefore, we first separated needleleaf and broadleaf forests from the forest cover map by the previous step, then separated each of these into evergreen and deciduous forests resulting in the four forest types listed above such as evergreen needleleaf forests.

To separate needleleaf and broadleaf forests, we overlaid all 11 data sets containing forest types over all eight study periods (Table 1), and a total of 29 data layers were included. According to the assumption mentioned above, two static consistency maps related to needleleaf and broadleaf forests were prepared by summing up all 29 data layers (Figure S4 in Supporting Information S1). First, similar to forest reconstruction, we also calculated the consistency (CON) of needleleaf forest (CON_{need}) and broadleaf forest (CON_{broa}) at each pixel, that is, the number of LULC data sets that identified the pixel as the needleleaf or broadleaf forest. At each pixel, there were two consistency indexes CON_{need} and CON_{broa}, and then we preferentially identified the needleleaf (broadleaf) forest at the pixels with $CON_{need} > CON_{broa}$ ($CON_{broa} > CON_{need}$) using the same method for identifying forest as above introduced. If the total area of identified needleleaf (broadleaf) forests does not meet the reported needleleaf (broadleaf) forest area of NFI, we prioritized the data to identify the dominant forest type from the remaining forest pixels and then identified another forest type. The dominant forest type in a given province is the forest type occupying the majority of the forest area according to the NFI. Theoretically, the total area of the two delineated forest types can identify the corresponding prescribed areas from NFI records; the remaining forest pixels will be considered as other forest types (bamboo and economically important plantation forests).

Similar to the reconstruction of needleleaf/broadleaf forest types, we further separated evergreen and deciduous forest types from needleleaf and broadleaf forest types, individually (Figure S5 in Supporting Information S1). Because no area records exist for evergreen and deciduous forest types of NFI data sets, we directly separated evergreen/deciduous needleleaf forest types from these needleleaf forest pixels, which were relatively consistently identified as evergreen/deciduous needleleaf forests, and similar operations were conducted for separating evergreen/deciduous broadleaf forest types from broadleaf forest pixels. The prior knowledge mentioned in Section 2.1.4 between climate zone and forest type was employed to further separate the evergreen/deciduous forest types from these remaining needleleaf and broadleaf forest pixels, individually.

2.3. Accuracy Assessment

We employed two different methods to validate the accuracy of the reconstructed forest cover maps, including field survey-based and consistency-based validation techniques (Fang et al., 2020). Initially, we randomly labeled 395 site-specific annual samples from 1985 to 2015 at 5-year intervals, based on very high spatial resolution images and archived Landsat time-series images (Figure 2). In addition, we collected 665 and 2791 third-party field surveys from the literature acquired in 2010 and 2015, respectively (Qin et al., 2015; Zhang et al., 2021). All 3851 field surveys were collected to obtain the confusion matrix of the reconstructed forest cover map for each period. The overall accuracy (OA) shows the proportion of all field surveys correctly classified. The producer's accuracy (PA) shows the proportion of surveyed truth samples properly classified as the target class, and the user's accuracy (UA) shows the proportion of samples classified as the target class on the classification map confirmed by field surveys.

Additionally, the reconstructed forest cover maps were generated by combining multiple LULC data sets; therefore, we indirectly examined the accuracy of the maps by analyzing the consistency between all LULC data sets. A reconstructed forest pixel was identified as forest cover by more LULC data sets (i.e., higher consistency), and then the reconstructed forest pixel had the larger confidence properly identified as the forest (Fang et al., 2020).

2.4. Analysis Methods

2.4.1. Consistency Analysis

Consistency was measured at each pixel and defined as the number of LULC data sets that identified a given pixel as a forest type (Gao et al., 2020). For instance, the consistency of three indicated that three out of all available LULC data sets classify the forest type the same at a given pixel. Therefore, the more consistent these LULC data sets are, the more likely this investigated pixel is actually a forest (Fang et al., 2020).

2.4.2. Forest Change Analysis

Forest change refers to the forest cover transitions between forest and non-forest during two successive time points, and can be classified into change (gain or loss) and non-change (stable forest or stable non-forest) events (Winkler et al., 2021). Forest gain is defined as the transition from non-forest to forest, and forest loss is the inverse of forest gain, from forest to non-forest (Hansen et al., 2013). During multi-successive time steps, forest gain and forest loss may occur successively. Therefore, the gross forest change from 1980 to 2015 includes three possible change events (forest gain, loss, gain, and loss), and the occurrence frequencies of gross forest change events represent the intensities of forest change.

3. Results

3.1. Accuracy Assessment of Reconstructed Forest Cover Data Set

This study reconstructed a new forest cover data set, called the Chinese Forest Cover Data set (CFCD), from 1980 to 2015 by combining several current LULC data sets. First, we used field surveys acquired from 1985 to 2015 covering seven study time points to examine the accuracy of data sets. Based on 395 site-specific field surveys, the validation shows that the OA increased over time, varied from 75.4% to 93.9%, and producer's and user's accuracies varied from 55.5% to 94.3% and from 93.6% to 97.3% for forest type (Table 2), respectively. In addition, based on the 665 and 2791 three-party field surveys acquired in 2010 and 2015, the validation shows the OA was 93.8% and 99.4%, producer's accuracy was 90.6% and 99.3%, and user's accuracy was 96.8% and 97.0% for forest type, respectively.

The confidence of CFCD was measured at each forest pixel and defined as the consistency among all LULC data sets. For all forests, there were 4, 4, 6, 5, 11, 8, 12, and 10 LULC data sets employed for reconstructing forest cover for all eight study time points. We found that there were 32%, 74%, 48%, 60%, 31%, 45%, 32%, and 35% of reconstructed forest pixels reaching the corresponding maximum consistency at eight study time points, respectively. The proportion of reconstructed forest pixels where the consistency is one was only 1% (Figure 3a). For forest types, we noted that the consistency of reconstructed broadleaf forests was larger than that of needleleaf forests (Figures 3b and 3c). Notably, there remain few (less than 4%) reconstructed needleleaf and broadleaf forest pixels having no consistency of corresponding forest type according to our method (Figures 3b and 3c).

3.2. Consistency Evaluation and Comparison of LULC Data Sets

Consistency between existing LULC data sets showed significant spatial variations. Low consistency mainly occurred in Northwest China and along the east coast of China (Figure 4). The former was attributed to a harsh natural environment and sparse forest cover, which create challenges to the identification of forest types by remote sensing, such as in Xinjiang, Qinghai, and Ningxia provinces. The latter was attributed to dense population and scattered forest cover, such as that in Tianjin, Shandong, Jiangsu, and Shanghai provinces. High consistency mainly concentrated in Heilongjiang, Jilin, Zhejiang, Fujian, and Taiwan provinces, all of which had a high percentage of forest cover.

We also compared the correlation between forest area statistics derived from NFI data and forest area estimations derived from LULC data sets at the provincial scale where wide discrepancies were observed (Figure 5).

Table 2
Confusion Matrix of Reconstructed Forest Cover Map From 1985 to 2015

		Classification				
Year	Reference	Forest	Non-forest	User's accuracy	Producer's accuracy	Overall accuracy
1985	Forest	116	93	96.7%	55.5%	75.4%
	Non-forest	4	182	66.2%	97.9%	
1990	Forest	150	59	96.2%	71.8%	83.6%
	Non-forest	6	180	75.3%	96.8%	
1995	Forest	165	45	96.5%	78.6%	87.1%
	Non-forest	6	179	79.9%	96.8%	
2000	Forest	183	26	97.3%	87.6%	92.2%
	Non-forest	5	181	87.4%	97.3%	
2005	Forest	191	20	93.6%	90.5%	91.7%
	Non-forest	13	171	89.5%	92.9%	
2010	Forest	199	12	94.3%	94.3%	93.9%
	Non-forest	12	172	93.5%	93.5%	
2015	Forest	197	13	94.3%	93.8%	93.7%
	Non-forest	12	173	93.0%	93.5%	
2010[a]	Forest	300	31	96.8%	90.6%	93.8%
	Non-forest	10	324	91.3%	97.0%	
2015[a]	Forest	415	3	97.0%	99.3%	99.4%
	Non-forest	13	2360	99.9%	99.5%	

[a]Indicates field survey data available from Qin et al. (2015) and Zhang et al. (2021), respectively.

Compared with NFI, the majority of LULC data sets tended to overestimate the forest area; this tendency was more frequent during the early periods, especially before 1990.

3.3. Spatial and Temporal Changes of Forest Cover

The spatial pattern of forest cover derived from CFCD was basically consistent among various time points from 1980 to 2015 (Figure 6, Figure S6 in Supporting Information S1). Spatially, Northeast, Southeast, and Southwest China were the main forest distribution areas, while sparse forest cover occurred in Northwest, Central China, and East China. In addition, evergreen needleleaf forests were mainly located in South China, whereas deciduous

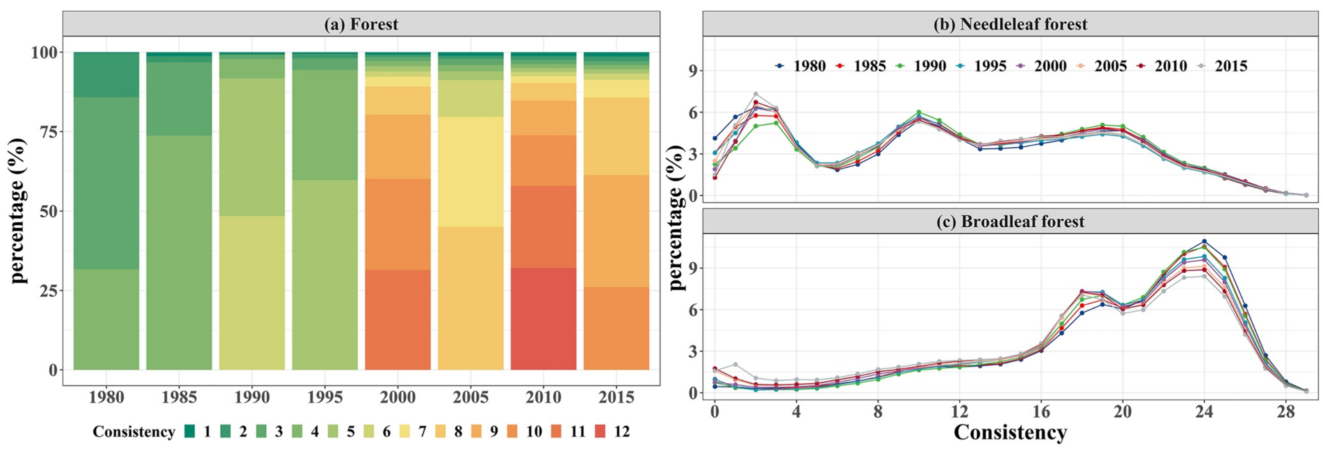

Figure 3. Consistency-based confidence of the Chinese Forest Cover Data set, based on 5-year intervals from 1980 to 2015.

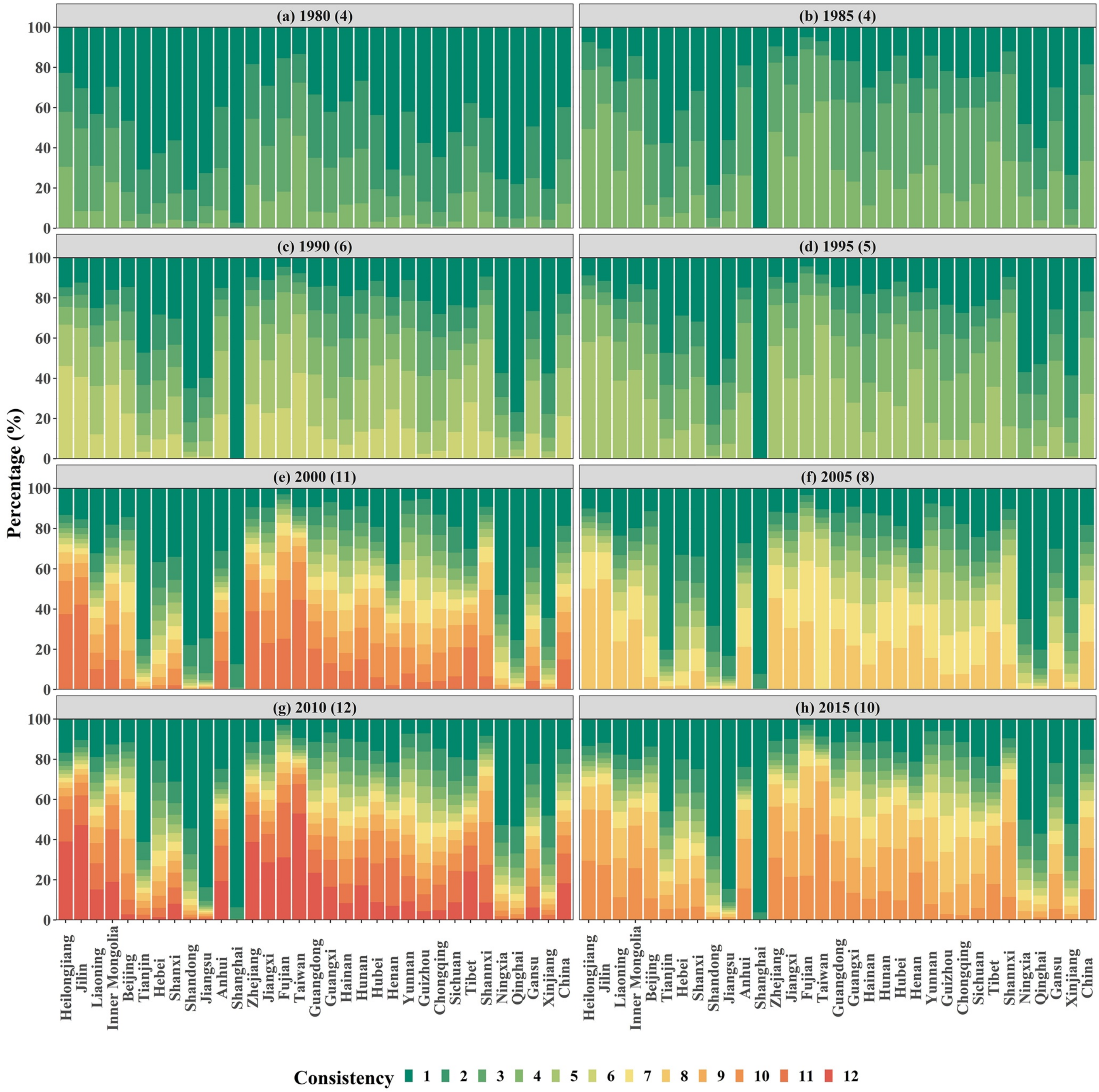

Figure 4. Consistency between all land use and land cover (LULC) data sets for 32 provincial administrative regions and for China as a whole in (a) 1980; (b) 1985; (c) 1990; (d) 1995; (e) 2000; (f) 2005; (g) 2010; (h) 2015. The numbers in parentheses after the year indicate the amount of LULC data sets involved.

needleleaf forests were concentrated in Northeast China. The evergreen broadleaf forests occurred preferentially in South China, while deciduous broadleaf forests were mainly distributed in Northeast China.

Temporally, the CFCD data set can reproduce the long-term changes of forest cover in China very well (Figure 7). The forest cover area in China has increased from 115×10^4 km^2 in 1980 to 205×10^4 km^2 in 2015 with a growth rate of 2.2% yr^{-1} according to the NFI data. The forest area estimations derived from the CFCD data set show a rate of increase that is close to that based on forest area statistics derived from NFI. In addition, the CFCD data set also can accurately indicate the temporal changes of the two broadly defined forest types (broadleaf and needleleaf forests) since the 1980s. In contrast, the available LULC data sets failed to reproduce the historical changes of forest cover in China since the 1980s (Figure 7). Almost all data sets underestimated the rate

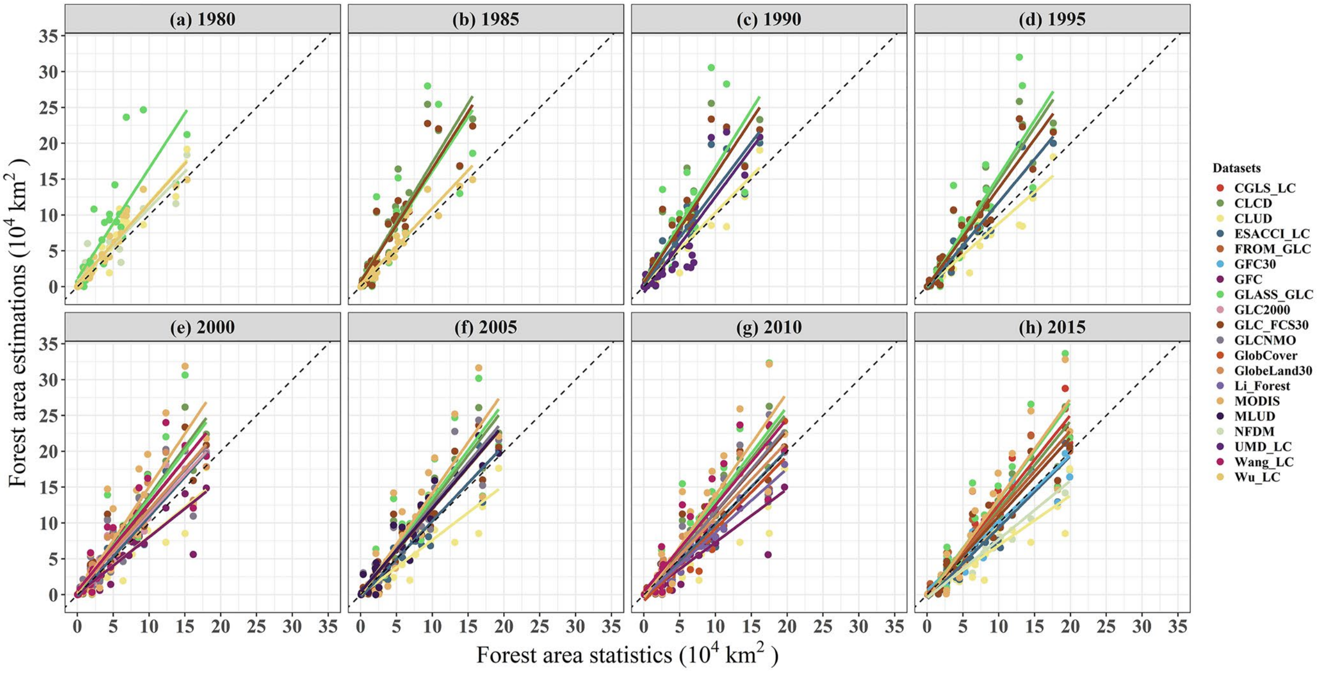

Figure 5. Scatter plots between forest areas statistics derived from National Forest Inventory data and forest areas estimations derived from land use and land cover data at the provincial/administrative unit scale at the following points in time: (a) 1980; (b) 1985; (c) 1990; (d) 1995; (e) 2000; (f) 2005; (g) 2010; (h) 2015.

of increase for forest cover. For example, the CLUD data set showed a constant forest cover area from 1980 to 2015 but did not indicate the forest gains that have been a benefit of afforestation projects in China. Although the GLASS_GLC data set also showed a comparable forest gain in China, the forest area estimations were much higher than the forest area statistics from NFI. Additionally, the existing LULC data set. also failed to reproduce historical variations of needleleaf and broadleaf forests (Figures 7b and 7c).

The gross forest change extent from 1980 to 2015 was 153 × 10^4 km^2, which accounts for 16% of the total land surface in China (Figure 8a). Among all change events, 44% were only forest gain, 4% were forest loss only, and 52% were a mixture of forest gain and loss. The area of stable forest was 79 × 10^4 km^2, accounting for 69% of NFI forest area in 1980. This implies that 31% of the forest in 1980 has been lost. When considering the intensity

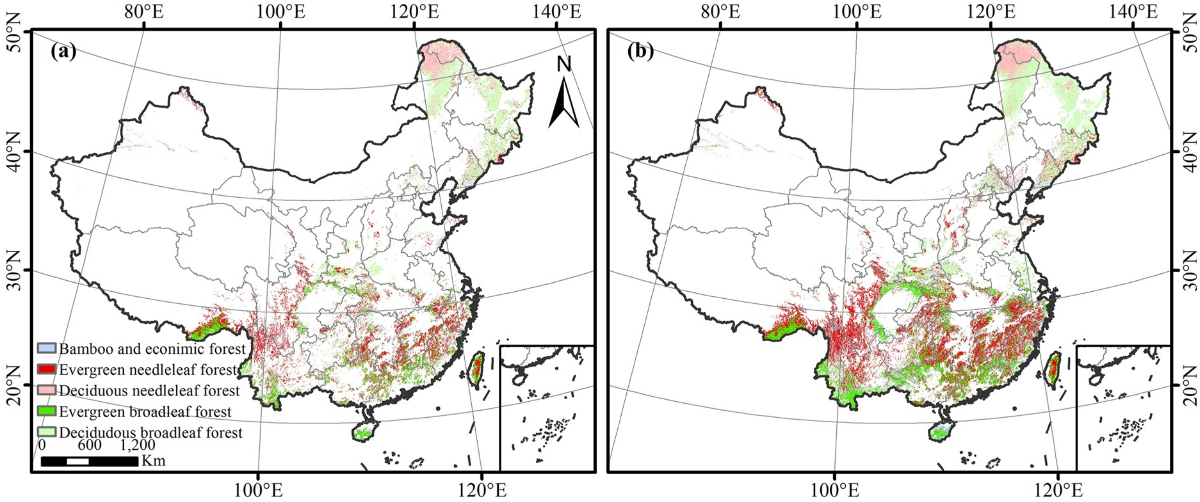

Figure 6. Spatial patterns of five types of forests in reconstructed forest cover maps in (a) 1980 and (b) 2015 including: bamboo and economically important plantation, evergreen needleleaf, deciduous needleleaf, evergreen broadleaf, and deciduous broadleaf forests.

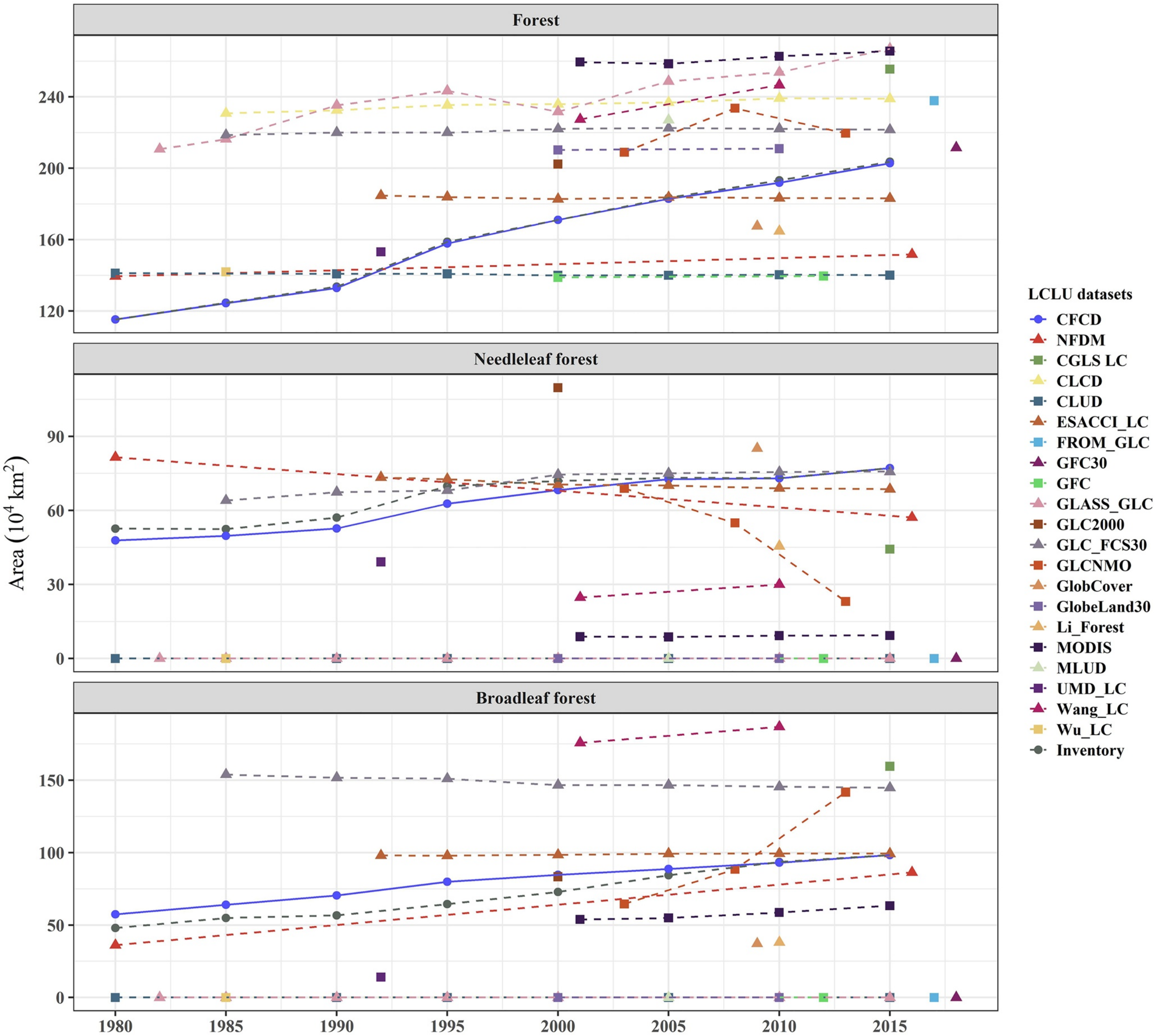

Figure 7. Temporal dynamics of forest area derived from National Forest Inventory and land use and land cover data sets for: (a) all forests; (b) needleleaf forests; (c) broadleaf forests.

of forest change, the hotspot for change mainly occurred in Southern China (Figure 8b). Among provinces, the highest forest change region was Fujian Province, and the lowest is Qinghai Province, where 53% and 0.7% of the land surface has changed at least once, respectively.

Except during 1990–1995, forest gain and forest loss simultaneously decreased in the past decades, resulting in a relatively stable net forest change (Figure 9a). The ratio of area of forest loss over forest gain indicates the relative intensity of afforestation or deforestation. A higher ratio (above 70%) was found before 1990 and a lower ratio (about 50%) was observed after 1995; this change was mainly attributable to intensified environmental protection, partly attributable to a lower accuracy of our CFCD before 1995. The rate of gross forest change was 4.4×10^4 km^2 per year based on our CDCF, and all other long-term LULC data sets underestimated the changes, from 26.6% for GLASS_GLC to 93.4% for CLUD (Figure 9b). Notably, very slight variations of forest area estimations (net forest change) versus considerable variations of forest gain and loss (gross forest change) observed in both the MODIS and GLC_FCS30 data sets, clearly demonstrate the difference between gross and net forest change, because gross change is important for the carbon estimation model (Houghton, 2020; Yue et al., 2018).

10.1029/2022JG007101

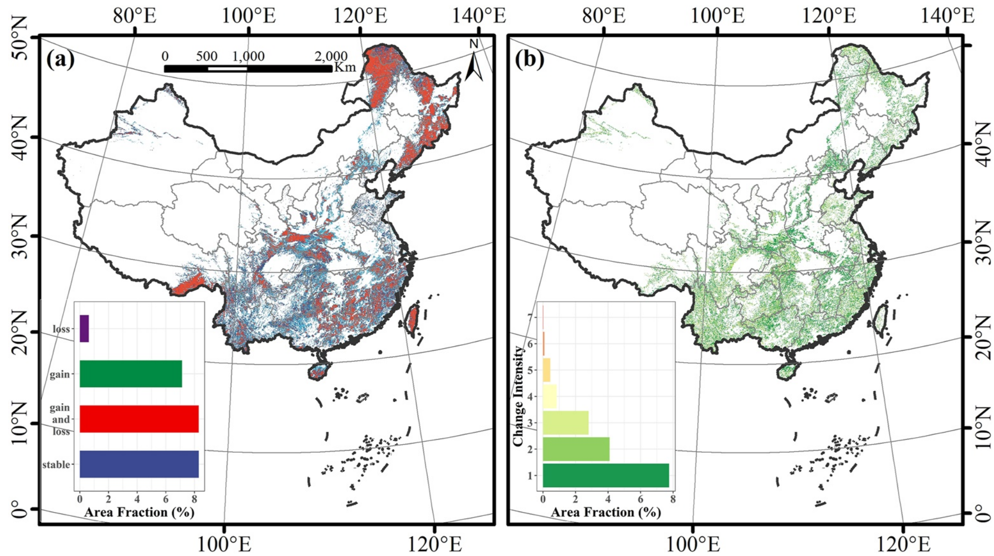

Figure 8. Spatial patterns of (a) gross forest change (gain, loss, and gain and loss) and (b) forest change intensity during the entire period of this study (1980–2015).

4. Discussion

As one of the most important types of ecosystems, forests play a dominant role in determining the extent of the terrestrial carbon sink in China (Liu et al., 2014). Forest carbon sinks offer a cost-effective pathway to offset fossil-fuel emissions, and even provide the main pathway to achieving a goal of carbon neutrality (Cai et al., 2022; Griscom et al., 2017). Especially during the most recent decades, numerous afforestation projects have been implemented across large regions in China, so forest coverage has increased to 23% currently from 12% in the early 1980s according to NFI data set (State Forestry Bureau, 2019). Another national census of land cover, national land survey, also shows a substantial increase of forest area through 2009 to 2019 (Chen et al., 2022), which is quite close to the increased area derived from NFI data set. Therefore, quantifying the contributions of increased forest coverage to the terrestrial carbon sink is quite important in China (Lu et al., 2018). However, the current LULC data sets failed to reproduce temporal changes of forest coverage during the past decades (Figure 7), which may be one of the largest uncertainties when quantifying carbon sinks in China (Li et al., 2016). Given that the existing LULC data set underestimated the increased rate of forest coverage, the current estimates of the carbon sink based on these LULC data sets may actually underestimate the enhanced contributions of forests in China.

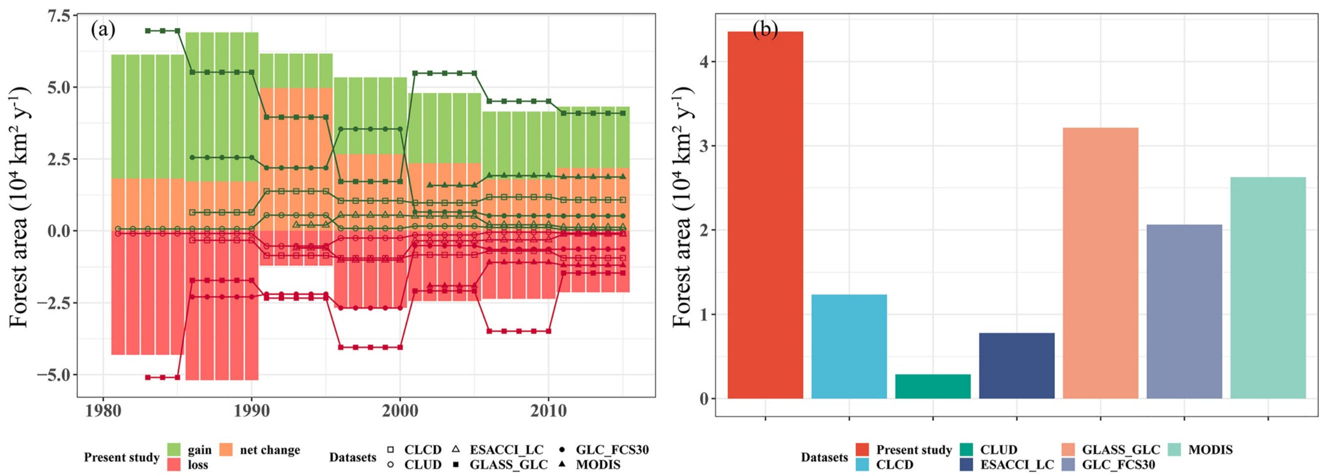

Figure 9. Comparison of (a) trends and (b) rates of forest change between long-term land use and land cover data sets during the study period.

10.1029/2022JG007101

The present study highlighted the fact that the currently available LULC data sets little reproduce long-term changes of forest coverage consistent with NFI in China. In particular, all LULC projections, except GLASS_GLC, greatly underestimated the increase in the spatial extent of forests (Figure 7). Especially, our results highlighted that these LULC data sets highly underestimated forest change (Figures 7 and 9). According to NFI data, the forest area has increased from 115×10^4 km^2 in the early 1980s to 220×10^4 km^2 around 2015 (State Forestry Bureau, 2019), suggesting only the afforestation results in the land cover change over about 11% of total land surface in China. While, the deforestation must also occur since the 1980s, and therefore, the percentage of gross forest change must be higher than 11%. This study selected 7 data sets covering more than 14 years to investigate their performance for indicating gross forest change. GLASS_GLC data set showed the largest gross forest change, accounting for 11.05% of total land surface in China since 1980, which was close to the percentage resulting from afforestation only. The gross forest change derived from other 6 data sets only accounted for 1.04%–6.44% (Figure 9b). Underestimated forest change will underestimate the impacts of forest change on carbon and water cycles of terrestrial ecosystems in China (Schwärzel et al., 2020; Yu et al., 2022). The CFCD data set developed by this study showed the gross forest change extent from 1980 to 2015 was 153×10^4 km^2, 16% of the total land surface in China. It is urgently needed to evaluate the impacts of forest change based on this new data set.

Most satellite-based LULC data sets used machine learning methods to classify vegetation types (Friedl et al., 2010; Gong et al., 2019; Zhang et al., 2021). Although machine learning classification methods have become popular for mapping land cover, the accuracy highly depends on the representativeness, quantity, and quality of the training samples employed (Liu et al., 2020). Due to the inadequacy of long-term very high spatial resolution images as reference data, labeling adequate training samples across different years remains challenging (Pengra et al., 2020). Therefore, the model trained by current training samples was directly applied for classifying historical land cover characteristics; this alternative method called transfer learning has been proven to work well where the land cover did not witness a significant change (Gong et al., 2019). However, it is not suitable for applying transfer learning to map historical forest cover change directly, since China experienced unprecedented afforestation from the 1980s. Owing to the unrepresentative training data, a model trained by samples with stable land cover has little capacity to capture this forest change in China (Yang & Huang, 2021). High consistency of data sources and annual training samples improve the performance of long-term land cover mapping, especially for change analysis (Liu et al., 2020; Xu et al., 2018). Moreover, the satellite-based signature difference across space is much more significant than that across time. Therefore, capturing temporal dynamics of land cover remains more challenging than revealing spatial variation.

This study generated a long-term new forest cover data set (i.e., CFCD) by combining 20 prevailing LULC data sets; CFCD can reproduce the long-term forest cover changes that have occurred in China since the 1980s when compared with NFI data (Figure 7). In addition, we analyzed the long-term changes in the connectivity of forest pixels since the 1980s. Connected forest landscapes, in general, indicate better ecosystem service values (Camba Sans et al., 2021). We discovered that solitary forest patches with only one pixel accounted for 0.30% of all pixels in 1985 and 0.86% in 1990; small forest patches with an area of fewer than 100 pixels accounted for about 10% during 1980–2015 (Figure 10). As the area of forest grows, so does the area of each forest patch, and more small forest patches will merge to form larger forest patches.

Some potential uncertainties could affect the accuracy of forest identification. First, the inherent uncertainties of existing data sets are propagated into the newly developed data set. Basically, two types of classification errors exist: errors of omission (i.e., missed forest pixel) and commission (i.e., overestimated forest pixel) in the existing data sets. These existing data sets use different definitions of forests (Table S1 in Supporting Information S1), which highly determines the forest area. NFI defines forest as tree cover >20% and coverage area >667 m^2. However, most data sets define forest with less tree cover (e.g., tree cover >15% for CGLS_LC data set) (Table S1 in Supporting Information S1). Therefore, most data sets showed larger forest area estimations than those derived from the NFI data set (Figure 7). The higher consistency of forest identification among these data sets indicates a better performance of this data set (Fang et al., 2020). Our results showed that there was a high consistency of identification among various data sets over most provinces. However, over several provinces, such as Shanghai and Tianjin, the consistency was still low, which may imply the low performance over these provinces.

Second, our data set shows a lower identification accuracy in the 1980s and 1990s when compared with those after 2000 (Table 2, Figure 3). The accuracy of forest reconstruction highly depends on the numbers and accuracy

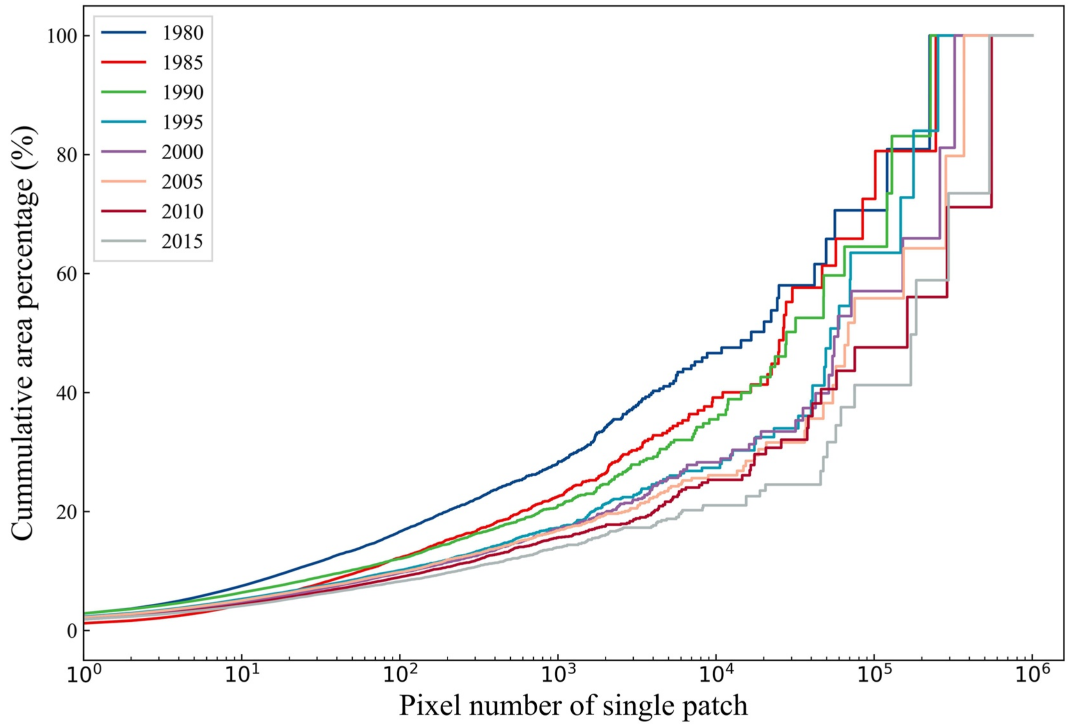

Figure 10. Cumulative distribution of the pixel number of forest patches in China at 5-year intervals for 1985 to 2015.

of available forest cover maps; the more forest cover maps that are available, the more confident the forest reconstruction is (Fang et al., 2020). The limited number of available LULC data sets before 2000 resulted in a relatively low accuracy in our forest reconstruction product. Data availability (especially satellite remote sensing data) is the essential precondition for large-scale land cover mapping (Liu et al., 2021). Before 2000, Landsat-4/5 and NOAA AVHRR were rarely limited choices for mapping land cover, and those also are the main data sources in CLUD, CLCD, ESA CCI-LC, and GLASSGLC data sets. After 2000, increasing available remote sensing data (especially Landsat-7 and MODIS) and free data sharing greatly facilitated land cover mapping studies. Several recent studies highlighted that the number of cloud-free satellite images largely determines how well the seasonal change of a vegetation index can be retrieved, thus impacting the map accuracy (Shen et al., 2022; Zheng et al., 2022). Most products are produced based on Landsat data sets. However, the availability of free-cloud imagery during the late periods is better than that during the early periods (Pengra et al., 2020), especially the launch of Landsat-7 in 1999 greatly mitigates the imagery limitation of Landsat archives (Wulder et al., 2016). Additionally, the availability of very high spatial resolution images (including aerial photographs) also helped to provide more essential ground samples for land cover mapping (Pengra et al., 2020). Google Earth Engine software, with a vast data archive and powerful computation, provides a new opportunity in land cover mapping fields, but inadequate ground samples still constrain any attempt to generate land cover products covering before 2000 (Tamiminia et al., 2020).

Third, the accuracy of CFCD highly depends on the NFI data. China has already developed an integrated forest inventory system that provides valuable information for forest coverage. However, the accuracy of NFI also is strongly impacted by the inventory method, number and representativeness of ground sample plots (Lei et al., 2009). Especially, there are large differences in accuracy of NFI over the various periods because of evolution of sampling design and method (Lei et al., 2009). For example, the fourth NFI (1989–1993) started to use both ground and remote sensing samples to calculate provincial forest area, and especially since the sixth NFI (1999–2003) the number of remote sensing samples substantially increase, which largely improve the accuracy of NFI data (Lei et al., 2009). Any uncertainties of NFI data will be propagated into the CFCD. Our study may imply the underestimation of forest coverage by CFCD because of lower producer's accuracy in the early periods (Table 2). On contrary, the producer's accuracy in the late periods is much higher (i.e., >90% after 2000). In addition, the inversed thresholds in the several provinces derived by this method are not reliable, which implies the non-negligible uncertainties of this method over several provinces. For example, the consistence threshold of Shandong in 2010 is zero (Figure S3g in Supporting Information S1), suggesting the identified forest areas from all LULC data sets are less than the forest area derived from NFI. The different accuracy of NFI data over the regional scale may be an important reason. Besides large heterogeneity of samples among the various periods, there are also spatial heterogeneity of samples (Lei et al., 2009). This study did not made efforts to identify forest coverage in these provinces, and thus CFCD generated in this study underestimated forest area compared with NFI data.

Finally, a spatial resolution of 0.01° cannot meets the requirements of fine resolution research, such as identifying areas of forest fragmentation (Morreale et al., 2021) and forest degradation (Chen et al., 2021). A coarse resolution indicates the existence of mixed pixels that will obscure forest patches with a small area. Of course, forest reconstruction also can generate a forest cover map with a 30 m resolution, but a 0.01° resolution is sufficient as forcing data for terrestrial ecosystem models.

5. Conclusions

We produced accurate forest cover map data sets covering 1980 to 2015, and reproduced forest spatial-temporal dynamics consistent with NFI records by combining multi-source data sets. Most available LULC data sets generally overestimate forest cover area and meanwhile underestimate the rate of gross forest change. Inconsistency among existing LULC data sets limits their usefulness for inter-comparison and further application. Forest reconstruction has been proven to have a huge potential to provide consistent forest cover maps that researchers can be confident in using; the reconstruction idea, mainly including forest probability based on consistency analysis and the application of prior knowledge, such as forest inventory records and the correlation between climate zone maps and forest type, can be applied for other fields.

Data Availability Statement

The land use and land cover data sets used in this paper are collected from the corresponding reference in Table 1. The forest inventory records are accessible from the National Forestry and Grassland Data Center of China (http://www.forestdata.cn/).

Acknowledgments

This work was supported by a key project of the National Natural Science Foundation of China (Grants 42141020; 31930072). X. Xiao is supported by the U.S. National Science Foundation (1911955). This organization was not involved in the design of this study. The forest inventory records are accessible from the National Forestry and Grassland Data Center of China.

References

Bartholomé, E., & Belward, A. S. (2005). GLC2000: A new approach to global land cover mapping from Earth observation data. *International Journal of Remote Sensing*, *26*(9), 1959–1977. https://doi.org/10.1080/01431160412331291297

Bontemps, S., Defourny, P., Bogaert, E. V., Arino, O., Kalogirou, V., & Perez, J. R. (2010). GLOBCOVER 2009 products description and validation report. Retrieved from http://due.esrin.esa.int/files/GLOBCOVER2009_Validation_Report_2.2.pdf

Buchhorn, M., Lesiv, M., Tsendbazar, N.-E., Herold, M., Bertels, L., & Smets, B. (2020). Copernicus global land cover layers—Collection 2. *Remote Sensing*, *12*(6), 1044. https://doi.org/10.3390/rs12061044

Cai, W., He, N., Li, M., Xu, L., Wang, L., Zhu, J., et al. (2022). Carbon sequestration of Chinese forests from 2010 to 2060: Spatiotemporal dynamics and its regulatory strategies. *Science Bulletin*, *67*(8), 836–843. https://doi.org/10.1016/j.scib.2021.12.012

Camba Sans, G. H., Verón, S. R., & Paruelo, J. M. (2021). Forest strips increase connectivity and modify forests' functioning in a deforestation hotspot. *Journal of Environmental Management*, *290*, 112606. https://doi.org/10.1016/j.jenvman.2021.112606

Chen, J., Chen, J., Liao, A., Cao, X., Chen, L., Chen, X., et al. (2015). Global land cover mapping at 30m resolution: A POK-based operational approach. *ISPRS Journal of Photogrammetry and Remote Sensing*, *103*, 7–27. https://doi.org/10.1016/j.isprsjprs.2014.09.002

Chen, S., Woodcock, C. E., Bullock, E. L., Arévalo, P., Torchinava, P., Peng, S., & Olofsson, P. (2021). Monitoring temperate forest degradation on Google Earth Engine using Landsat time series analysis. *Remote Sensing of Environment*, *265*, 112648. https://doi.org/10.1016/j.rse.2021.112648

Chen, X., Yu, L., Du, Z., Liu, Z., Qi, Y., Liu, T., & Gong, P. (2022). Toward sustainable land use in China: A perspective on China's national land surveys. *Land Use Policy*, *123*, 106428. https://doi.org/10.1016/j.landusepol.2022.106428

ESA. (2014). Land cover CCI: Product user guide version 2. Retrieved from http://maps.elie.ucl.ac.be/CCI/viewer/download/ESACCI-LC-Ph2-PUGv2_2.0.pdf

Fang, J., Chen, A., Peng, C., Zhao, S., & Ci, L. (2001). Changes in forest biomass carbon storage in China between 1949 and 1998. *Science*, *292*(5525), 2320–2322. https://doi.org/10.1126/science.1058629

Fang, J., Yu, G., Liu, L., Hu, S., & Chapin, F. S. (2018). Climate change, human impacts, and carbon sequestration in China. *Proceedings of the National Academy of Sciences of the United States of America*, *115*(16), 4015–4020. https://doi.org/10.1073/pnas.1700304115

Fang, X., Zhao, W., Zhang, C., Zhang, D., Wei, X., Qiu, W., & Ye, Y. (2020). Methodology for credibility assessment of historical global LUCC datasets. *Science China Earth Sciences*, *63*(7), 1013–1025. https://doi.org/10.1007/s11430-019-9555-3

FAO. (2016). State of the world's forests 2016. Forests and agriculture: Land-use challenges and opportunities.

Friedl, M. A., Sulla-Menashe, D., Tan, B., Schneider, A., Ramankutty, N., Sibley, A., & Huang, X. (2010). MODIS collection 5 global land cover: Algorithm refinements and characterization of new datasets. *Remote Sensing of Environment*, *114*(1), 168–182. https://doi.org/10.1016/j.rse.2009.08.016

Friedlingstein, P., O'Sullivan, M., Jones, M. W., Andrew, R. M., Hauck, J., Olsen, A., et al. (2020). Global carbon budget 2020. *Earth System Science Data*, *12*(4), 3269–3340. https://doi.org/10.5194/essd-12-3269-2020

Gao, Y., Liu, L., Zhang, X., Chen, X., Mi, J., & Xie, S. (2020). Consistency analysis and accuracy assessment of three global 30-m land-cover products over the European Union using the LUCAS dataset. *Remote Sensing*, *12*(21), 3479. https://doi.org/10.3390/rs12213479

Ge, Y., Jia, Y., Chen, Y., Xu, X., Jiang, D., & Zhang, D. (2018). A multi-scale provincial land use dataset of the Chinese mainland based on super-resolution mapping. *Journal of Global Change Data & Discovery*, *2*(3), 323–330. https://doi.org/10.3974/geodp.2018.03.11

Gong, P., Liu, H., Zhang, M., Li, C., Wang, J., Huang, H., et al. (2019). Stable classification with limited sample: Transferring a 30-m resolution sample set collected in 2015 to mapping 10-m resolution global land cover in 2017. *Science Bulletin*, *64*(6), 370–373. https://doi.org/10.1016/j.scib.2019.03.002

Griscom, B. W., Adams, J., Ellis, P. W., Houghton, R. A., Lomax, G., Miteva, D. A., et al. (2017). Natural climate solutions. *Proceedings of the National Academy of Sciences of the United States of America*, *114*(44), 11645–11650. https://doi.org/10.1073/pnas.1710465114

Hansen, M. C., Defries, R. S., Townshend, J. R. G., & Sohlberg, R. (2000). Global land cover classification at 1 km spatial resolution using a classification tree approach. *International Journal of Remote Sensing*, *21*(6–7), 1331–1364. https://doi.org/10.1080/014311600210209

Hansen, M. C., Potapov, P. V., Moore, R., Hancher, M., Turubanova, S. A., Tyukavina, A., et al. (2013). High-resolution global maps of 21st-century forest cover change. *Science*, *342*(6160), 850–853. https://doi.org/10.1126/science.1244693

Houghton, R. A. (2020). Terrestrial fluxes of carbon in GCP carbon budgets. *Global Change Biology*, *26*(5), 3006–3014. https://doi.org/10.1111/gcb.15050

Houghton, R. A., Hobbie, J. E., Melillo, J. M., Moore, B., Peterson, B. J., Shaver, G. R., & Woodwell, G. M. (1983). Changes in the carbon content of terrestrial biota and soils between 1860 and 1980: A net release of CO"2 to the atmosphere. *Ecological Monographs*, *53*(3), 235–262. https://doi.org/10.2307/1942531

Houghton, R. A., & Nassikas, A. A. (2018). Negative emissions from stopping deforestation and forest degradation, globally. *Global Change Biology*, *24*(1), 350–359. https://doi.org/10.1111/gcb.13876

Lei, X. D., Tang, M. P., Lu, Y. C., Hong, L. X., & Tian, D. L. (2009). Forest inventory in China: Status and challenges. *International Forestry Review*, *11*(1), 52–63. https://doi.org/10.1505/ifor.11.1.52

Le Noë, J., Erb, K.-H., Matej, S., Magerl, A., Bhan, M., & Gingrich, S. (2021). Altered growth conditions more than reforestation counteracted forest biomass carbon emissions 1990–2020. *Nature Communications*, *12*(1), 6075. https://doi.org/10.1038/s41467-021-26398-2

Li, C., Wang, J., Hu, L., Yu, L., Clinton, N., Huang, H., et al. (2014). A Circa 2010 thirty meter resolution forest map for China. *Remote Sensing*, *6*(6), 5325–5343. https://doi.org/10.3390/rs6065325

Li, P., Zhu, J., Hu, H., Guo, Z., Pan, Y., Birdsey, R., & Fang, J. (2016). The relative contributions of forest growth and areal expansion to forest biomass carbon. *Biogeosciences*, *13*(2), 375–388. https://doi.org/10.5194/bg-13-375-2016

Lin, G., Wen, X., Zhou, C., & She, G. (2013). Review and progress of China's forest continuous inventory system. *Open Journal of Forestry*, *03*(01), 17–22. https://doi.org/10.4236/ojf.2013.31004

Liu, D., Chen, Y., Cai, W., Dong, W., Xiao, J., Chen, J., et al. (2014). The contribution of China's grain to green program to carbon sequestration. *Landscape Ecology*, *29*(10), 1675–1688. https://doi.org/10.1007/s10980-014-0081-4

Liu, H., Gong, P., Wang, J., Clinton, N., Bai, Y., & Liang, S. (2020). Annual dynamics of global land cover and its long-term changes from 1982 to 2015. *Earth System Science Data*, *12*(2), 1217–1243. https://doi.org/10.5194/essd-12-1217-2020

Liu, J., Liu, M., Tian, H., Zhuang, D., Zhang, Z., Zhang, W., et al. (2005). Spatial and temporal patterns of China's cropland during 1990–2000: An analysis based on Landsat TM data. *Remote Sensing of Environment*, *98*(4), 442–456. https://doi.org/10.1016/j.rse.2005.08.012

Liu, L., Zhang, X., Gao, Y., Chen, X., Shuai, X., & Mi, J. (2021). Finer-resolution mapping of global land cover: Recent developments, consistency analysis, and prospects. *Journal of Remote Sensing*, *2021*, 1–38. https://doi.org/10.34133/2021/5289697

Lu, F., Hu, H., Sun, W., Zhu, J., Liu, G., Zhou, W., et al. (2018). Effects of national ecological restoration projects on carbon sequestration in China from 2001 to 2010. *Proceedings of the National Academy of Sciences of the United States of America*, *115*(16), 4039–4044. https://doi.org/10.1073/pnas.1700294115

Morreale, L. L., Thompson, J. R., Tang, X., Reinmann, A. B., & Hutyra, L. R. (2021). Elevated growth and biomass along temperate forest edges. *Nature Communications*, *12*(1), 7181. https://doi.org/10.1038/s41467-021-27373-7

NDRC. (2021). Working guidance for carbon dioxide peaking and carbon neutrality in full and faithful implementation of the new development philosophy. Retrieved from https://en.ndrc.gov.cn/policies/202110/t20211024_1300725.html

Pan, Y., Birdsey, R. A., Fang, J., Houghton, R., Kauppi, P. E., Kurz, W. A., et al. (2011). A large and persistent carbon sink in the world's forests. *Science*, *333*(6045), 988–993. https://doi.org/10.1126/science.1201609

Pengra, B. W., Stehman, S. V., Horton, J. A., Dockter, D. J., Schroeder, T. A., Yang, Z., et al. (2020). Quality control and assessment of interpreter consistency of annual land cover reference data in an operational national monitoring program. *Remote Sensing of Environment*, *238*, 111261. https://doi.org/10.1016/j.rse.2019.111261

Piao, S., Fang, J., Ciais, P., Peylin, P., Huang, Y., Sitch, S., & Wang, T. (2009). The carbon balance of terrestrial ecosystems in China. *Nature*, *458*(7241), 1009–1013. https://doi.org/10.1038/nature07944

Qin, Y., Xiao, X., Dong, J., Zhang, G., Shimada, M., Liu, J., et al. (2015). Forest cover maps of China in 2010 from multiple approaches and data sources: PALSAR, landsat, MODIS, FRA, and NFI. *ISPRS Journal of Photogrammetry and Remote Sensing*, *109*, 1–16. https://doi.org/10.1016/j.isprsjprs.2015.08.010

Rogelj, J., Schaeffer, M., Meinshausen, M., Knutti, R., Alcamo, J., Riahi, K., & Hare, W. (2015). Zero emission targets as long-term global goals for climate protection. *Environmental Research Letters*, *10*(10), 105007. https://doi.org/10.1088/1748-9326/10/10/105007

Ryan, M. G., & Law, B. E. (2005). Interpreting, measuring, and modeling soil respiration. *Biogeochemistry*, *73*(1), 3–27. https://doi.org/10.1007/s10533-004-5167-7

Schepaschenko, D., See, L., Lesiv, M., McCallum, I., Fritz, S., Salk, C., et al. (2015). Development of a global hybrid forest mask through the synergy of remote sensing, crowdsourcing and FAO statistics. *Remote Sensing of Environment*, *162*, 208–220. https://doi.org/10.1016/j.rse.2015.02.011

Schwärzel, K., Zhang, L., Montanarella, L., Wang, Y., & Sun, G. (2020). How afforestation affects the water cycle in drylands: A process-based comparative analysis. *Global Change Biology*, *26*(2), 944–959. https://doi.org/10.1111/gcb.14875

Shen, R., Dong, J., Yuan, W., Han, W., Ye, T., & Zhao, W. (2022). A 30 m resolution distribution map of maize for China based on landsat and sentinel images. *Journal of Remote Sensing*, *2022*, 1–12. https://doi.org/10.34133/2022/9846712

State Forestry Bureau. (2003). Technical regulation for national forestry inventory. Retrieved from https://www.docin.com/p-2502302986.html

State Forestry Bureau. (2019). *China forest resources report in 2014-2018*. China Forestry Publishing.

Tamiminia, H., Salehi, B., Mahdianpari, M., Quackenbush, L., Adeli, S., & Brisco, B. (2020). Google Earth engine for geo-big data applications: A meta-analysis and systematic review. *ISPRS Journal of Photogrammetry and Remote Sensing*, *164*, 152–170. https://doi.org/10.1016/j.isprsjprs.2020.04.001

Tang, X., Zhao, X., Bai, Y., Tang, Z., Wang, W., Zhao, Y., et al. (2018). Carbon pools in China's terrestrial ecosystems: New estimates based on an intensive field survey. *Proceedings of the National Academy of Sciences of the United States of America*, *115*(16), 4021–4026. https://doi.org/10.1073/pnas.1700291115

Tateishi, R., Uriyangqai, B., Al-Bilbisi, H., Ghar, M. A., Tsend-Ayush, J., Kobayashi, T., et al. (2011). Production of global land cover data—GLCNMO. *International Journal of Digital Earth*, *4*(1), 22–49. https://doi.org/10.1080/17538941003777521

Wang, J., Zhao, Y., Li, C., Yu, L., Liu, D., & Gong, P. (2015). Mapping global land cover in 2001 and 2010 with spatial-temporal consistency at 250m resolution. *ISPRS Journal of Photogrammetry and Remote Sensing*, *103*, 38–47. https://doi.org/10.1016/j.isprsjprs.2014.03.007

Winkler, K., Fuchs, R., Rounsevell, M., & Herold, M. (2021). Global land use changes are four times greater than previously estimated. *Nature Communications*, *12*(1), 2501. https://doi.org/10.1038/s41467-021-22702-2

Wulder, M. A., White, J. C., Loveland, T. R., Woodcock, C. E., Belward, A. S., Cohen, W. B., et al. (2016). The global Landsat archive: Status, consolidation, and direction. *Remote Sensing of Environment*, *185*, 271–283. https://doi.org/10.1016/j.rse.2015.11.032

Xu, Y., Yu, L., Zhao, F. R., Cai, X., Zhao, J., Lu, H., & Gong, P. (2018). Tracking annual cropland changes from 1984 to 2016 using time-series Landsat images with a change-detection and post-classification approach: Experiments from three sites in Africa. *Remote Sensing of Environment*, *218*, 13–31. https://doi.org/10.1016/j.rse.2018.09.008

Yang, J., & Huang, X. (2021). The 30 m annual land cover dataset and its dynamics in China from 1990 to 2019. *Earth System Science Data*, *13*(8), 3907–3925. https://doi.org/10.5194/essd-13-3907-2021

Yu, Z., Ciais, P., Piao, S., Houghton, R. A., Lu, C., Tian, H., et al. (2022). Forest expansion dominates China's land carbon sink since 1980. *Nature Communications*, *13*(1), 5374. https://doi.org/10.1038/s41467-022-32961-2

Yuan, W., Li, X., Liang, S., Cui, X., Dong, W., Liu, S., et al. (2014). Characterization of locations and extents of afforestation from the grain for green project in China. *Remote Sensing Letters*, *5*(3), 221–229. https://doi.org/10.1080/2150704X.2014.894655

Yue, C., Ciais, P., Luyssaert, S., Li, W., McGrath, M. J., Chang, J., & Peng, S. (2018). Representing anthropogenic gross land use change, wood harvest, and forest age dynamics in a global vegetation model ORCHIDEE-MICT v8.4.2. *Geoscientific Model Development*, *11*(1), 409–428. https://doi.org/10.5194/gmd-11-409-2018

Zeng, W., Tomppo, E., Healey, S. P., & Gadow, K. V. (2015). The national forest inventory in China: History—Results—International context. *Forest Ecosystems*, *2*(1), 23. https://doi.org/10.1186/s40663-015-0047-2

Zhang, X., Liu, L., Chen, X., Gao, Y., Xie, S., & Mi, J. (2021). GLC_FCS30: Global land-cover product with fine classification system at 30 m using time-series Landsat imagery. *Earth System Science Data*, *13*(6), 2753–2776. https://doi.org/10.5194/essd-13-2753-2021

Zhang, X., Long, T., He, G., Guo, Y., Yin, R., Zhang, Z., et al. (2020). Rapid generation of global forest cover map using Landsat based on the forest ecological zones. *Journal of Applied Remote Sensing*, *14*(02), 1. https://doi.org/10.1117/1.JRS.14.022211

Zheng, Y., Li, Z., Pan, B., Lin, S., Dong, J., Li, X., & Yuan, W. (2022). Development of a phenology-based method for identifying sugarcane plantation areas in China using high-resolution satellite datasets. *Remote Sensing*, *14*(5), 1274. https://doi.org/10.3390/rs14051274